# IMPACT OF MATERIAL TYPE ON STRUCTURAL ANALYSIS PERFORMED ON TWO WING CASES

Constantin Cristian ANDREI[1], Constantin - Stelian STAN[2], Iuliana STAN[3]

*The purpose of this research is to determine which of the two alloys of magnesium and aluminum is superior as a material for an ONERA M6 wing that can be utilized during subsonic flight in a compressible regime. With this wing, CFD numerical simulations were performed for a variety of angles of attack (AoA) and the pressures that resulted from the simulations for each AoA were used to make a static structural analysis. The results show that even though the Mg alloy has a lower density than the Al alloy, the von Misses equivalent stress that occurs on an Al alloy wing resulted from fluid-structure interaction does not exceed the proportionality limit, in contrast to the case of the Mg alloy wing, which for high AoA passes into the plastic domain of the material.*

**Keywords**: ONERA M6, 2024T3 aluminum alloy, WE43A-T6 magnesium alloy, CFD analysis, static structural analysis

## 1. Introduction

When it comes to the design process of a wing, the selection of the material to be used is of the utmost importance. While designing the wing, engineers need to make sure that the material that is used is not only lightweight but also has a high level of resistance to twisting and bending. As a result, the aim of this paper was to investigate two different cases of wing. The first case is a wing made of 2024T3 aluminum alloy (Aluminum alloyed mostly with Copper and Magnesium, heat treated), and the second is a WE43A-T6 magnesium alloy wing (Magnesium alloyed with Neodymium and Ytterbium, heat treated) [1]. The French national aerospace research institute ONERA (Office National d'Etudes et de Recherches Aérospatiales) oversees the development of the experimental model of the wing which is being simulated in both cases. This model is known as the ONERA M6 [2], shown in Figure 1. The wing geometry was adopted from AGARD AR-138 [3], whose data is shown in Table 1.

[1] Eng., National Institute for Aerospace Research "Elie Carafoli" – INCAS Bucharest, Romania, e-mail: andrei.cristian@incas.ro
[2] Prof., Dept. of Material Science and Engineering, National University of Science and Technology POLITEHNICA Bucharest, Romania, e-mail: constantin.stan@upb.ro
[3] Lect., Dept. of Material Science and Engineering, National University of Science and Technology POLITEHNICA Bucharest, Romania, e-mail: iuliana.stan@upb.ro

*Table 1*

**ONERA M6 wing geometry data [2]**

| | |
|---|---|
| Wing Semi Span, m | 1.1963 |
| Mean aerodynamic center, m | 0.64607 |
| Aspect ratio | 3.8 |
| Taper ratio | 0.56 |
| Leading edge sweep angle, deg | 30 |
| Trailing edge sweep angle, deg | 15.8 |
| Sweep angle at 25% chord, deg | 26.7 |


Fig.1. ONERA M6 wing model [2]

The work is divided into three stages: the first stage consists of a material analysis, in which are analyzed the wing materials used in this research, the second stage represents a CFD analysis, which involves solving the flow problem around the wing for a range of AoA from 0 to 16 degrees, and the third and final stage consists of a static structural analysis, during which the maximum deformation at the wing tip is determined using the pressures obtained in the CFD analysis, as well as the maximum stress that occur at the wing root. The ANSYS software was used to carry out the CFD and static structural numerical simulations.

## 2. Work methodology

### 2.1. Material analysis

Since low weight materials are widely used in aerospace industry, in this research two different types of lightweight alloy wings are compared, to find out which one is superior as a material for a wing that can be utilized in a compressible subsonic flight regime. The materials used in this research are: 2024T3 aluminum alloy and WE43A-T6 magnesium alloy.

### 2.1.1. 2024T3 aluminum alloy

2024T3 aluminum alloy is a 2024 aluminum alloy in the T3 temper, which belongs to the Al-Cu-Mg alloy group. It widely consists of aluminum and is alloyed with copper, as the primary alloying element, and other small amounts of other elements, including magnesium and manganese, as shown in Table 2. Copper is used as the main alloying element, due to the fact of providing strength to the alloy, while other elements contribute to many other properties, including corrosion resistance.

*Table 2*

**2024T3 aluminum alloy composition [1]**

| Al (%) | Cu (%) | Mg (%) | Mn (%) | Si (%) | Fe (%) | Zn (%) | Zr (%) | Ti (%) | Cr (%) | Residuals |
|---|---|---|---|---|---|---|---|---|---|---|
| 90.7 – 94.7 | 3.8 – 4.9 | 1.2 – 1.8 | 0.3 – 0.9 | 0 – 0.5 | 0 – 0.5 | 0 – 0.25 | 0 – 0.2 | 0 – 0.15 | 0 – 0.1 | 0 – 0.15 |

2024T3 aluminum alloy is part of 2000 series aluminum alloys, which are characterized by good mechanical properties, good weldability and workability and good corrosion resistance. As a result, they are widely used in the aerospace industry, for structural components, including wing spars, aircraft skin, or other critical parts, that are subject to mechanical stress or thermal shocks [4] [5] [6] [12] - [15].

### 2.1.2. WE43A-T6 magnesium alloy

WE43A-T6 magnesium alloy is a magnesium alloy composed of magnesium (Mg), yttrium (Y) and rare earth elements, as shown in Table 3. The alloy is in the T6 temper, where the alloy is heat-treated and artificially aged.

*Table 3*

**WE43A-T6 magnesium alloy composition [1]**

| Mg (%) | Y (%) | Zr (%) | Zn (%) | Li (%) | Mn (%) | Cu (%) | Si (%) | Fe (%) | Ni (%) | Other rare earths (%) | Residuals |
|---|---|---|---|---|---|---|---|---|---|---|---|
| 89.5 – 93.5 | 3.7 – 4.3 | 0.4 – 1 | 0 – 0.2 | 0 – 0.2 | 0 – 0.15 | 0 – 0.03 | 0 – 0.01 | 0 – 0.01 | 0 – 0.005 | 2.4 – 4.4 | 0 – 0.3 |

WE43A-T6 magnesium alloy is widely used in aerospace industry where lightweight materials are required. It provides good corrosion resistance and is suitable for applications where weight reduction is crucial.

## 2.2. CFD analysis

The computational fluid dynamics (CFD) analysis is divided into three stages: the first is to construct the geometry; the second is to generate the grid; and the third is to solve the flow problem. The geometry sketch was accomplished using ANSYS Design Modeler, which is included in ANSYS software. The fluid domain that enclosures the wing was designed as a hemisphere after the wing had been sketched out first (Fig. 2). The dimensions of the hemisphere were 10 chords upstream and 10 chords downstream.

After that, another domain was designed downstream of the wing to get more accurate data in the wake area, created as a result of the interaction between the fluid and the wing structure. Then, the final geometry is imported into ANSYS Meshing, to generate the grid. The boundary layer was built up from 30 layers with a growth rate of 1.08 to provide more precise results in the area surrounding the wing. After the construction of the grid, 1,400,000 cells and 240,000 nodes were obtained. The grid is depicted in Fig. 3.

To find the solution of the flow problem, the resulted grid was imported into ANSYS Fluent. The flow problem is based on solving the Navier-Stokes flow equations and turbulence model equations [7].

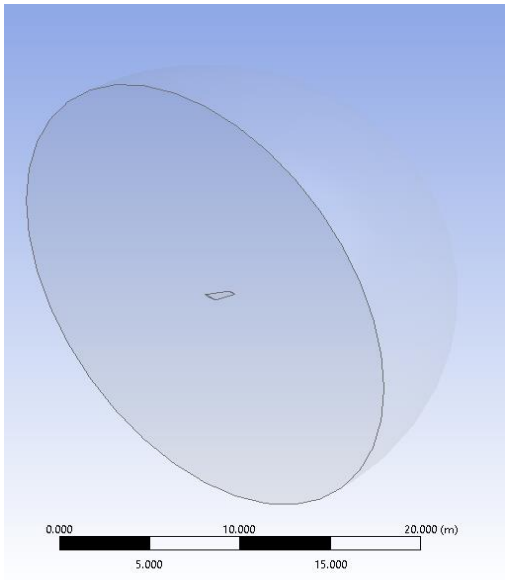


Fig. 2 Fluid domain in ANSYS Design Modeler

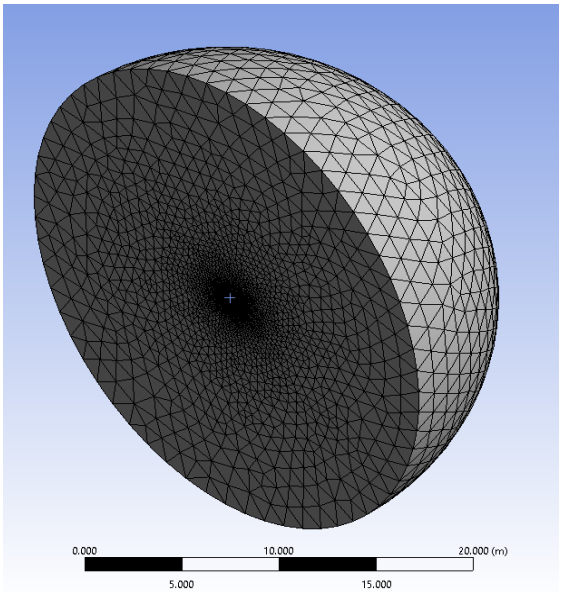


Fig. 3 Fluid domain mesh in ANSYS Meshing

As a result of compressibility effects, density is time-dependent, leading to the following flow equations:

$$\frac{\partial \rho}{\partial t} + \nabla(\rho \cdot V) = 0 \tag{1}$$

$$\frac{\partial}{\partial t}(\rho \cdot V) - \rho \cdot f + \nabla\left[-\overline{\overline{\sigma}} + (\rho \cdot V) \otimes V\right] = 0 \tag{2}$$

$$\frac{\partial}{\partial t}(\rho E) + \nabla(\rho H V) = \rho f V + q_v + \nabla\left(\kappa \nabla T + V\overline{\overline{\tau}}\right) \tag{3}$$

, where $\rho$ is density, is $V$ fluid volume, $f$ is external force, $\overline{\overline{\sigma}}$ is stress tensor, $E$ is total energy, $H$ is enthalpy, $q_v$ is heat source, $\kappa$ is thermic conductivity, $T$ is temperature, $v$ is molecular kinematic viscosity and $\mu$ is molecular dynamic viscosity [7].

The one-equation Spalart – Allmaras turbulence model was chosen as it involves the solution of only one transport equation, for kinematic turbulent viscosity [7] [8]. The main advantage of using the Spalart – Allmaras turbulence model is the lower computational effort compared to the widely used two-equation turbulence models [9]. To solve the flow problem, initial and boundary conditions were set, as following:

*Table 4*

**Reference values in ANSYS Fluent for initial and boundary conditions**

| | |
|---|---|
| Area, $m^2$ | 0.7532 |
| Density, $kg/m^3$ | 4.307524 |
| Enthalpy, J/kg | -6705.399 |
| Length, m | 0.64607 |
| Pressure, Pa | 3.1598e+5 |
| Temperature, K | 255.556 |
| Velocity, m/s | 268.9347 |
| Viscosity, kg/ms | 1.627716e-5 |
| Ratio of Specific Heats | 1.4 |
| Y+ for Heat Transfer Coefficient | 300 |

After setting up the turbulence model and the implementation of the initial and boundary conditions, a convergence criterion of $10^{-6}$ was imposed. Following the initialization of the flow problem, 500-time steps were set in order to compute the final solution. After the convergence criterion was fulfilled, the pressures measured on the wing were imported into ANSYS Static Structural to determine the maximum amount of deformation that could take place at the wing tip as well as the amount of stress that could occur during flight for each AoA.

## 2.3. Static structural analysis

Due to the non-stationary nature of the structural analysis performed in this work, the response of the wing material to external stress is not time dependent. The finite element method (FEM) approach was utilized in order to design a grid, used to compute the maximum amount of deformation at the wing tip. The main purpose of FEM is to investigate the structural behavior of a solid domain under the applications of the loads [10][11]. The force vector, stiffness matrix and mass matrix for each element are determined in the mesh generation. The relationship between force and displacement, as well as inertia force and acceleration for each element of the mesh can be computed using the following relations:

$$\left(\mathbf{f}_s\right)_e = \mathbf{k}_e \mathbf{u}_e \tag{12}$$

$$\left(\mathbf{f}_I\right)_e = \mathbf{m}_e \ddot{\mathbf{u}}_e \tag{13}$$

, where $\mathbf{k}_e$ is the stiffness matrix of the element, $\mathbf{m}_e$ is the mass matrix of the element, $\mathbf{u}_e$ is the displacement vector of the element and $\ddot{\mathbf{u}}_e$ is the acceleration vector of the element.

The displacement for each element can be determined by using the fluid – structure interaction equation [10][11], which is highlighted from the basic governing equation of motion, as follows:

$$[M]\{\ddot{U}\} + [C]\{\dot{U}\} + [K]\{U\} = \mathbf{p}(t) \tag{14}$$

, where $M$ is the structural mass matrix, $\ddot{\mathbf{U}}$ is the structural acceleration vector, $C$ is the structural dumping matrix, $\dot{\mathbf{U}}$ is the structural velocity vector, $K$ is the structural stiffness matrix, $\mathbf{U}$ is the displacement vector and $\mathbf{p}(t)$ is the force vector in a function of time.

To get more accurate results, it was necessary to build a fine grid of the wing, represented in Fig. 4, with 80,000 elements.

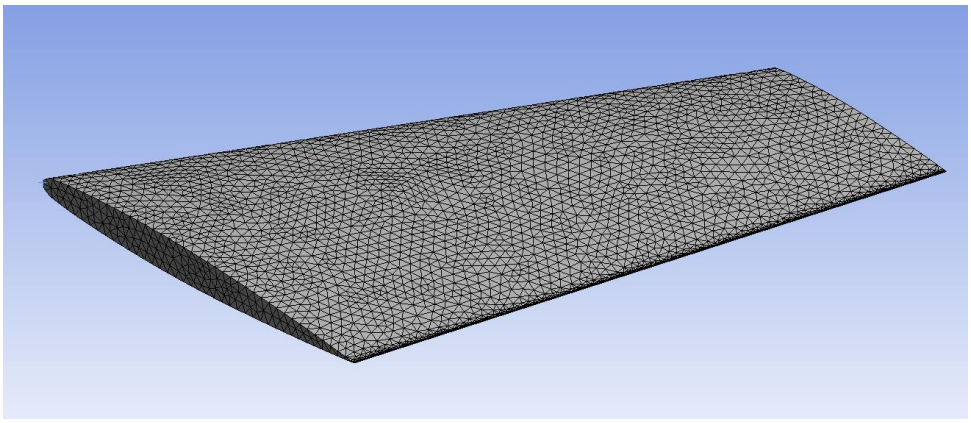

Fig. 4 Wing mesh for static structural analysis

Many numerical simulations were run for each AoA that was chosen, for both wing cases, in which predefined material properties are represented in Table 5.

*Table 5*

**Material properties [4]**

| Material type | 2024T3 Aluminum alloy | WE43A-T6 Magnesium alloy |
|---|---|---|
| Density, kg/m$^3$ | 3000 | 1900 |
| Young's Modulus, Pa | 7.1e10 | 4.4e10 |
| Poisson's ratio | 0.33 | 0.3 |
| Tensile Ultimate Strength, Pa | 4.8e8 | 2.5e8 |
| Yield Strength, Pa | 3.2e8 | 1.7e8 |

The entire work scheme is highlighted below, in Fig. 5. As mentioned before, it is divided into three stages: the first stage represents the material analysis, in which material properties are set, the second stage consists of a CFD analysis, which involves sketching the geometry of wing and fluid domain, creating the mesh and solving the flow problem around the wing for a range of AoA from 0 to 16 degrees, and the final stage is based on a static structural analysis, which consists of solving the maximum deformation of the wing using the pressure distribution on the wing, calculated in the first stage of CFD analysis, for two material cases, whose properties are mentioned in Table 5.

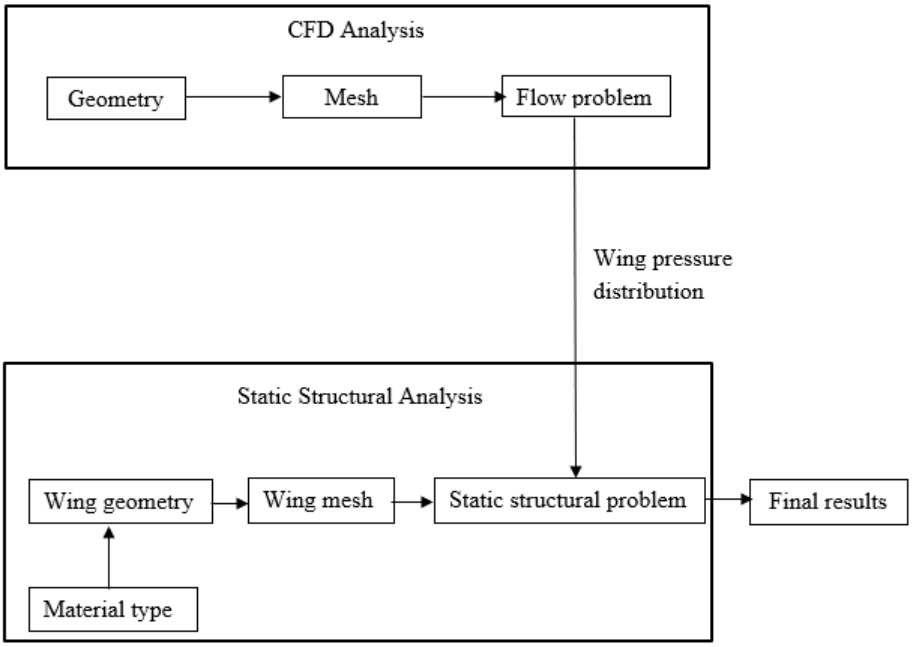


Fig. 5 Work Scheme

## 3. Results and conclusions

The increase of AoA will cause a pressure increase on the inner surface of the wing. The growth of the pressure from the inner surface of the wing leads to the increase of drag coefficient (Cd) and lift coefficient (Cl) to a maximum point, known as stall, beyond which the aircraft start to lose its control. The results of the numerical simulation indicate that stalling phenomenon, when the aircraft has a loss of responsiveness to control inputs, happens at an AoA of 14 degrees, according to Table 6.

*Table 6*

**CFD Results**

| AoA | Cl | Cd |
|---|---|---|
| 0 | 0 | 0.0083 |
| 2 | 0.2068 | 0.0122 |
| 4 | 0.4129 | 0.0272 |
| 6 | 0.5858 | 0.0532 |
| 8 | 0.7353 | 0.0901 |
| 10 | 0.8755 | 0.1371 |
| 12 | 0.9858 | 0.195 |
| 14 | 1.0522 | 0.262 |
| 16 | 0.945 | 0.391 |

It is also possible to observe that the increase of pressure that occurs as a result of the rise of AoA implies a growth of the maximum deformation that occurs at the wing tip (Fig. 6 – 8). Static structural results are highlighted in Table 7.

*Table 7*

**Static structural results**

| AoA | Maximum deformation (m) | | von Misses stress (Pa) | |
|---|---|---|---|---|
| | 2024T3 Al | WE43A-T6 | 2024T3 Al | WE43A-T6 |
| 0 | 1.88e-5 | 1.36e-5 | 1.87e7 | 3.17e6 |
| 2 | 5.8e-3 | 9.09e-3 | 3.33e7 | 3.36e7 |
| 4 | 1.21e-2 | 1.9e-2 | 6.86e7 | 6.93e7 |
| 6 | 1.83e-2 | 2.87e-2 | 1.02e8 | 1.03e8 |
| 8 | 2.7e-2 | 4.24e-2 | 1.45e8 | 1.46e8 |
| 10 | 3.38e-2 | 5.16e-2 | 1.75e8 | 1.72e8 |
| 12 | 3.61e-2 | 5.67e-2 | 1.93e8 | 1.94e8 |
| 14 | 3.89e-2 | 6.11e-2 | 2.09e8 | 2.11e8 |

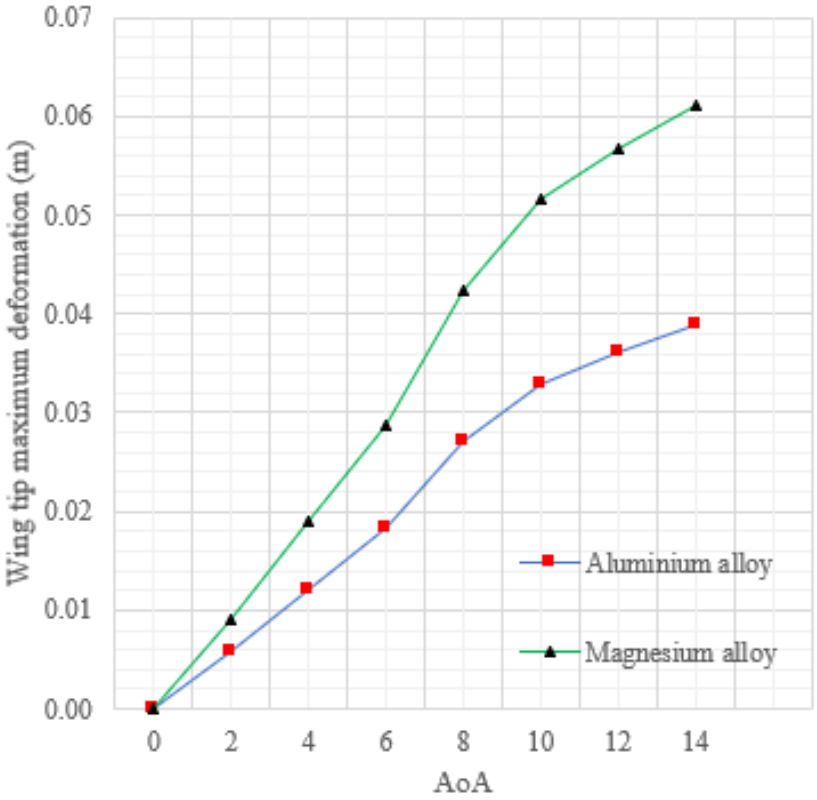


Fig. 6 Wing tip maximum deformation vs AoA

The exact nature of this increase depends on the material that was utilized. Due to the fact that Mg alloy has a lower density and a lower Young modulus than Al alloy, the wing made of Mg alloy has a higher maximum wing tip deformation per AoA than the wing made of Al alloy.

It is also possible to show that as AoA increases the von Misses equivalent stress will increase too, as depicted in Fig. 9 – 10.

Moreover, when the AoA for the wing made of Mg alloy increases beyond 10 degrees, the von Misses equivalent stress rises above the yield point of the material. As a result, the wing starts to begin to deform plastically.

As an important conclusion of this, even though WE43A-T6 magnesium alloy has a lower density than 2024T6 aluminum alloy, it is not recommended to use this type of alloy wing for high AoA, especially beyond 10 degrees as it enters into the plastic domain state.

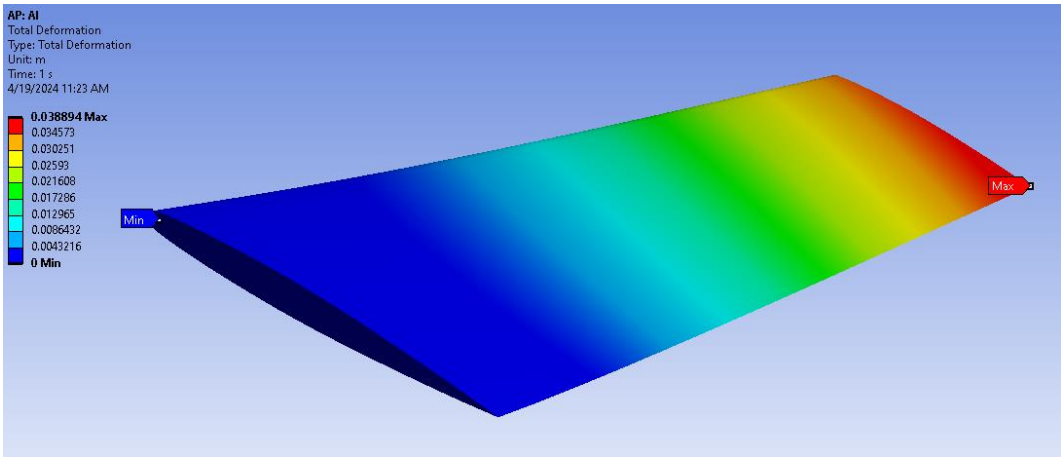


Fig. 7 Wing tip maximum deformation for Al alloy case for AoA = 14 deg

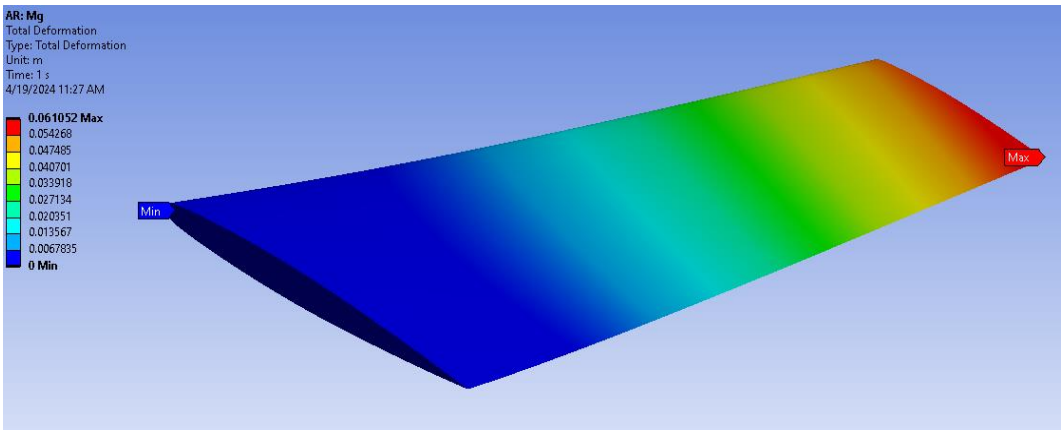


Fig. 8 Wing tip maximum deformation for Mg alloy case for AoA = 14 deg

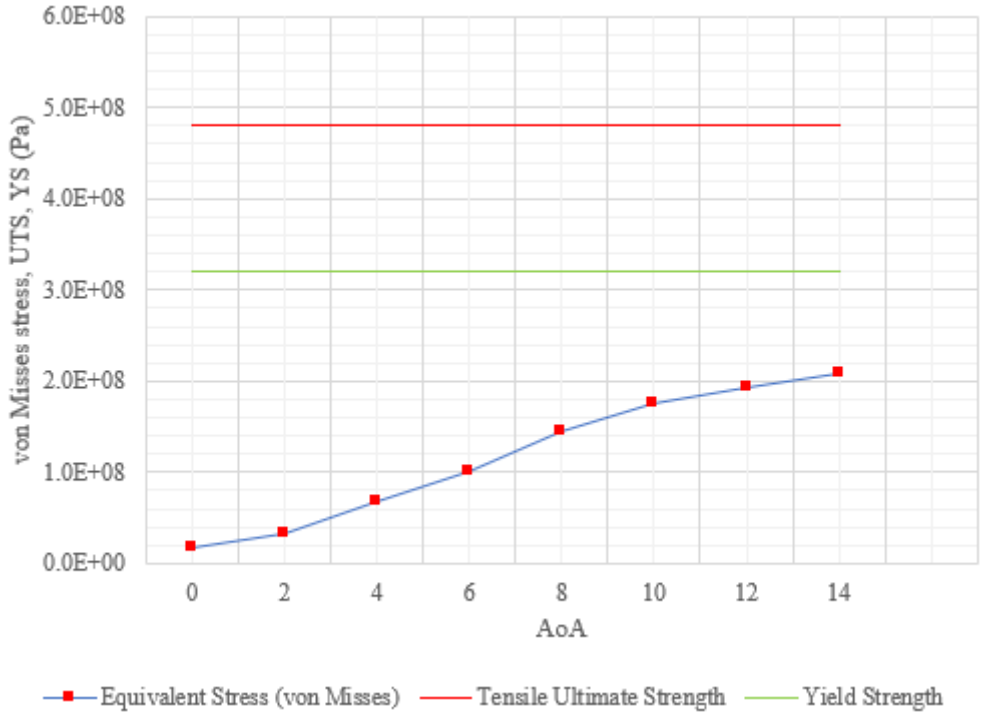


Fig. 9 Static structural results for 2024T3 Al alloy

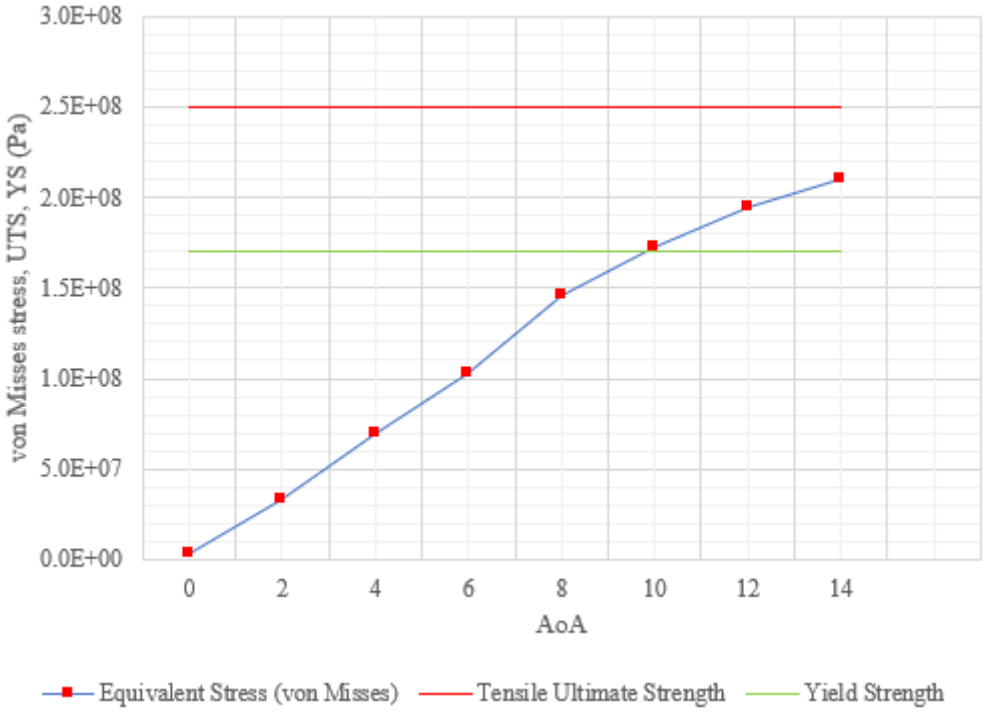


Fig. 10 Static structural results for WE43A-T6 Mg alloy

## R E F E R E N C E S

[1] *** Material Properties Database, https://www.makeitfrom.com/
[2] *** Langley Research Center Turbulence Modeling Resource. Turbulence modeling resource — 3D Onera M6 wing validation, https://turbmodels.larc.nasa.gov/onerawingnumerics_val.html.
[3] *V. Schmitt, F. Charpin*, "Pressure Distributions on the ONERA-M6-Wing at Transonic Mach Numbers", Experimental Data Base for Computer Program Assessment. Report of the Fluid Dynamics Panel Working Group 04, AGARD AR 138, May 1979
[4] *P.O. Odagiu, C.L. Salcianu, C. Ghera, A.D. Buzatu, L.M. Micu, A.N. Luca, I. Bordeasu, B. Ghiban*, "Heat treatment parameters influence on the cavitation resistance of an aluminum alloy", in UPB Scientific Bulletin, Series B, Vol. 85, Iss. 3, 2023
[5] *** Aircraft Aluminum Grades, https://matmatch.com/learn/material/aircraft-%20aluminum-grades.html
[6] *** Aluminium catalogue https://fdocumente.com/document/aluminiu-catalog.html
[7] *S. Danaila, M.S. Djeska*, Introducere in modelarea turbulentei (Introduction to turbulence modelling), Editura Politehnica Press, Bucuresti, 2017
[8] *P. Spalart, S. Allmaras*, A one-equation turbulence model for aerodynamic flows. Technical report AIAA Paper-92-0439, 1992
[9] *M.J.P. Razzaghi, S.M.R. Sani, Y. Masoumi, G. Huan*, "A Comparison of Various Turbulence Models for Analysis of Fluid Microjet Injection into the Boundary Layer over a Flat Surface", in Research Square Journal, 2022
[10] *R.S. Raja*, Coupled fluid structure interaction analysis on a cylinder exposed to ocean wave loading, Thesis, Chalmers University of Technology, Goteborg, Sweden, 2012
[11] *E.I. Basri, A.A. Basri, S. Balakrishnan, M.T.H.H. Sultan, K.A. Ahmad*, "Performance analysis of composite laminates wing skin with the aid of fluid structure interaction of aerodynamic loading-structural analysis", in Mechanics Based Design of Structures and Machines, 2022
[12] *F. Ştefănescu, G. Neagu, A. Mihai, Iuliana Stan*. Controlled Temperature Distribution and Heat Transfer Process in the Unidirectional Solidification of Aluminium Alloys, Advanced Materials and Structures IV, Book Series: Solid State Phenomena, Switzerland (97- 8-3-03785-391-7) Volume: 188, Pages: 314-317
[13] *G. Neagu, Fl. Ştefănescu, A. Mihai, Iuliana Stan, I. Odagiu*. Theoretical and Practical Aspects Regarding Al-SiC Particle Composites Obtained by Casting, Advanced Materials and Structures IV, Book Series: Solid State Phenomena, Switzerland (97- 8-3-03785-391-7) Volume: 188, Pages: 134-139
[14] *Stan, Iuliana; Stefanescu, Florin; Neagu, Gigel; Bogdan, Ovidiu*. Analysis by mathematical modelling of unidirectional solidification of aluminium, Scientific Bulletin of University "Politehnica" of Bucharest, Series B: Chemistry and Materials Science, 2015, Iss.2, ISSN 1454-2331, pp.143-154
[15] *I. Stan, Stelian Stan*, Influence of unidirectional solidification in Bridgman furnace on the mechanical behavior of a cast aluminum alloy, Scientific Bulletin of University "Politehnica" of Bucharest, Series B: Chemistry and Materials Science, 2017, Iss.2, ISSN 1454-2331, pp.143-154